Bremsstrahlung – low energy

Z. Was[*],

[*] Institute of Nuclear Physics, Krakow

- **(1)** For the simulation of decays of resonances bremsstrahlung must be taken into account. It is not separable because of infrared cancellations

For present day measurements precision is an issue: How bremsstrahlunh has to be included.

- **(2)** There is no underlying theory for bremsstrahlun from complex states like $\pi^\pm$ or $K^\pm$. For calulation of emission kernels used in reference predictions scalar QED is used. For detector simulations, so far universal kernel was used. It was good enough.

- **(3)**

- **(4)** Such an arrangement separates theoretical work and work on Monte Carlos used in experimental simulations of detector responses.

- **(5)** If needed form-factors may be added at a time of fits to the data. This is possible only if matrix element used in construction of kernel is explicitly available in a code. That is why kernels based on matrix elements are necessary.

... from my high energy talk of Sept 18 ...

For detector level studies simulation parts should communicate through event record:

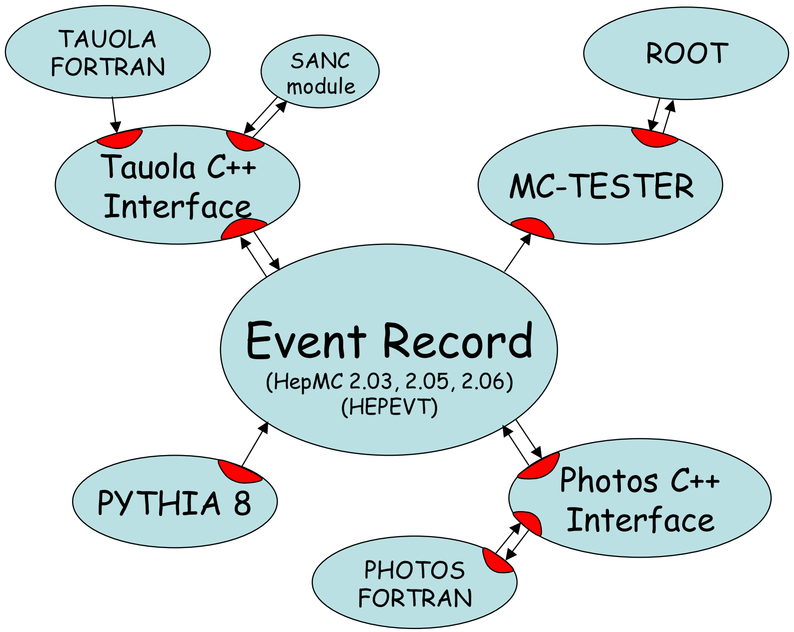

- Parts:

- hard process: (Born, weak, **new physics**),
- parton shower,
- τ decays
- QED bremsstrahlung

- High precision achieved

- Detector studies: acceptance, resolution lepton with or wihout photon.

Such organization requires:

- Good control of factorization (theory)
- Good understanding of tools on user side.

Matrix element applications for decay of hadronic resonances are so far in FORTRAN only.

Phase Space: exact

Orthodox exact Lorentz-invariant phase space (*Lips*) is in use in PHOTOS!

$$
\begin{aligned}
& dLips_{n+1}(P) = \\
& \frac{d^3k_1}{2k_1^0(2\pi)^3} \cdots \frac{d^3k_n}{2k_n^0(2\pi)^3} \frac{d^3q}{2q^0(2\pi)^3}(2\pi)^4\delta^4\Big(P - \sum_1^n k_i - q\Big) \\
= \quad & d^4p\delta^4(P-p-q)\frac{d^3q}{2q^0(2\pi)^3}\frac{d^3k_1}{2k_1^0(2\pi)^3} \cdots \frac{d^3k_n}{2k_n^0(2\pi)^3}(2\pi)^4\delta^4\Big(p - \sum_1^n k_i\Big) \\
= \quad & d^4p\delta^4(P-p-q)\frac{d^3q}{2q^0(2\pi)^3} dLips_n(p \to k_1 ... k_n).
\end{aligned}
$$

Integration variables, the four-vector p, compensated with $\delta^4\big(p - \sum_1^n k_i\big)$, and another integration variable M_1 compensated with $\delta\big(p^2 - M_1^2\big)$ are introduced.

Phase Space Formula of Photos

$$dLips_{n+1}(P \to k_1...k_n, k_{n+1}) = dLips_n^{+1\ tangent} \times W_n^{n+1},$$

$$dLips_n^{+1\ tangent} = dk_\gamma d\cos\theta d\phi \times dLips_n(P \to \bar{k}_1...\bar{k}_n),$$
$$\{k_1, \ldots, k_{n+1}\} = \mathbf{T}\big(k_\gamma, \theta, \phi, \{\bar{k}_1, \ldots, \bar{k}_n\}\big). \quad (1)$$

1. One can verify that if $dLips_n(P)$ was exact, then this formula lead to exact parametrization of $dLips_{n+1}(P)$
2. Practical implementation: Take the configurations from n-body phase space.
3. Turn it back into some coordinate variables.
4. construct new kinematical configuration from all variables.
5. **Forget about temporary** $k_\gamma \theta \phi$. **From now on, only weight and four vectors count.**
6. A lot depend on $\mathbf{T}$. Options depend on matrix element: must tangent at singularities. Simultaneous use of several $\mathbf{T}$ is possible and necessary/convenient if more than one charge is present in final state.

Phase Space: (main formula)

If we choose

$$G_n \;:\; M^2_{2\dots n}, \theta_1, \phi_1, M^2_{3\dots n}, \theta_2, \phi_2, \dots, \theta_{n-1}, \phi_{n-1} \;\longrightarrow\; \bar{k}_1 \dots \bar{k}_n \tag{2}$$

and

$$G_{n+1} \;:\; k_\gamma, \theta, \phi, M^2_{2\dots n}, \theta_1, \phi_1, M^2_{3\dots n}, \theta_2, \phi_2, \dots, \theta_{n-1}, \phi_{n-1} \;\longrightarrow\; k_1 \dots k_n, k_{n+1} \tag{3}$$

then

$$\mathbf{T} = G_{n+1}(k_\gamma, \theta, \phi, G_n^{-1}(\bar{k}_1, \dots, \bar{k}_n)). \tag{4}$$

The ratio of the Jacobians form the phase space weight W_n^{n+1} for the transformation. Such solution is universal and valid for any choice of G's. However, G_{n+1} and G_n has to match matrix element, otherwise algorithm will be inefficient (factor 10^{10} ...).

In case of PHOTOS G_n's

$$W_n^{n+1} = k_\gamma \frac{1}{2(2\pi)^3} \times \frac{\lambda^{1/2}(1, m_1^2/M^2_{1\dots n}, M^2_{2\dots n}/M^2_{1\dots n})}{\lambda^{1/2}(1, m_1^2/M^2, M^2_{2\dots n}/M^2)}, \tag{5}$$

Phase Space: (multiply iterated)

By iteration, we can generalize formula (1) and add l particles:

$$dLips_{n+l}(P \to k_1...k_n, k_{n+1}...k_{n+l}) = \frac{1}{l!}\prod_{i=1}^{l}\Big[dk_{\gamma_i} d\cos\theta_{\gamma_i} d\phi_{\gamma_i} W_{n+i-1}^{n+i}\Big]$$
$$\times dLips_n(P \to \bar{k}_1...\bar{k}_n), \qquad (6)$$
$$\{k_1,\ldots,k_{n+l}\} = \mathbf{T}\big(k_{\gamma_l},\theta_{\gamma_l},\phi_{\gamma_l},\mathbf{T}\big(\ldots,\mathbf{T}\big(k_{\gamma_1},\theta_{\gamma_1},\phi_{\gamma_1},\{\bar{k}_1,\ldots,\bar{k}_n\}\big)\ldots\big).$$

Note that variables $k_{\gamma_m}, \theta_{\gamma_m}, \phi_{\gamma_m}$ are used at a time of the $m-$th step of iteration only, and are not needed elsewhere in construction of the physical phase space; the same is true for invariants and angles $M^2_{2\ldots n}, \theta_1, \phi_1, \ldots, \theta_{n-1}, \phi_{n-1} \;\; \to \;\; \bar{k}_1 \ldots \bar{k}_n$ of (2,3), which are also redefined at each step of the iteration. Also intermediate steps require explicit construction of temporary $\bar{k}'_1 \ldots \bar{k}'_n \ldots \bar{k}'_{n+m}$, statistical factor $\frac{1}{l!}$ added.

We have **exact distribution** of **weighted** events over l and $n+l$ body phase spaces.

Status: practical

- PHOTOS feature complete exact phase space for multiphoton radiation.
- Unique double iteration algorithm: Internal loop is over emitting particles external one over consecutive photons: one can benefit from parton shower *and* exponentiation.
- for semileptonic decays there is only one highly boosted decay product. All other charged decay products are usually semi-relativistic only. Pre-sampler for collinear enhancement can be switched off for additional tests.
- To discuss theoretical systematics matrix element must be explicitly known and used in a code. Even if it is not of high theoretical accuracy it can be later modified with weight.
- PHOTOS offers such possiblity in few cases of non-leptonic decays.
- I will go over numerical examples from papers:

  Scalar QED, NLO and PHOTOS Monte Carlo G. Nanava, Z. Was, Eur.Phys.J. C51 (2007) 569-583

  Bremsstrahlung simulation in $K \to \pi l^{\pm} \nu_l (gamma)$ *decays* Qingjun Xu, Z. Was,Eur.Phys.J. C72 (2012) 2158

PHOTOS: main properties

$B^- \to \pi^0 K^-$: *standard PHOTOS* looks good, but ...

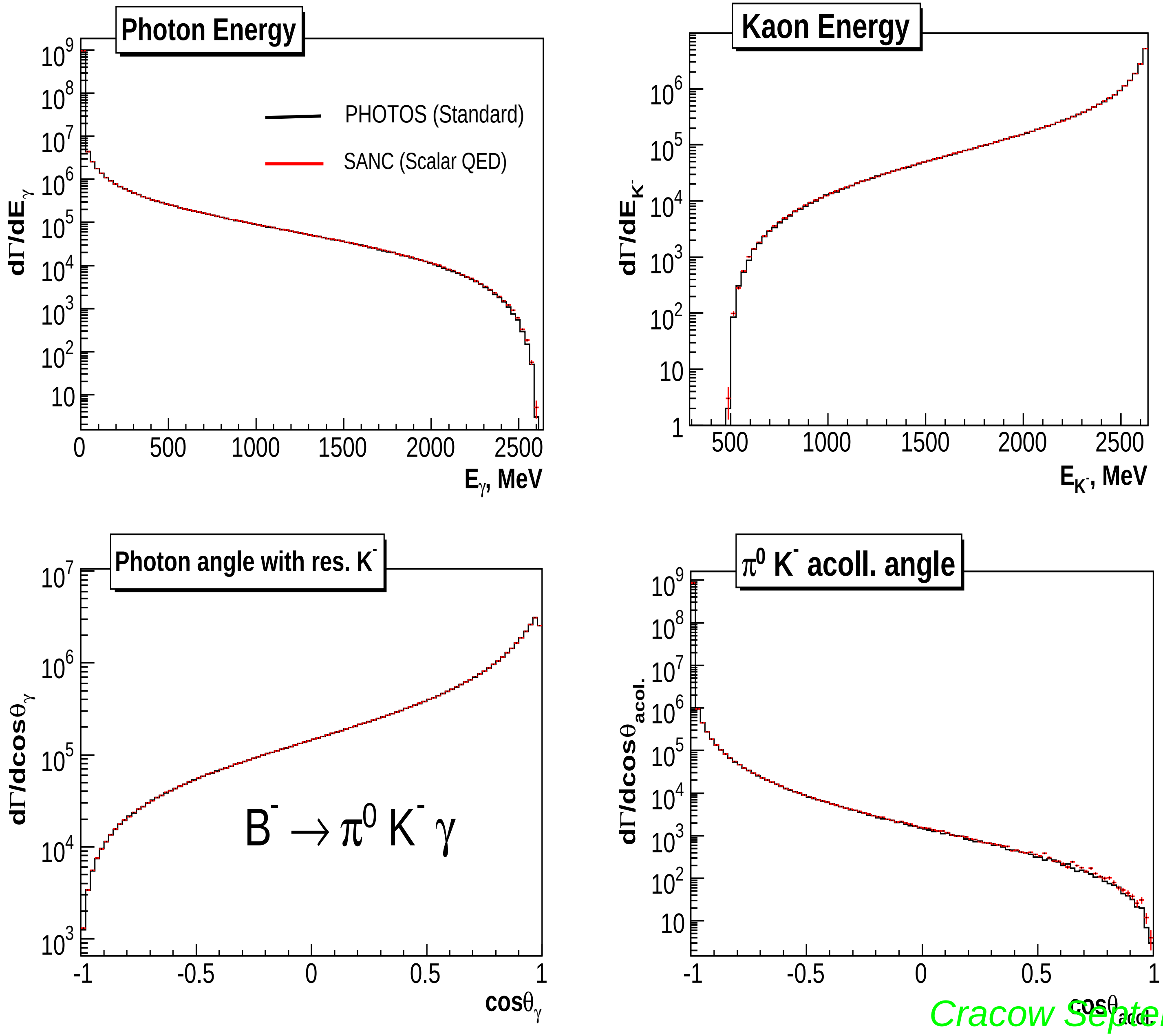

PHOTOS: main properties

$B^- \to \pi^0 K^-$: *standard PHOTOS* not perfect

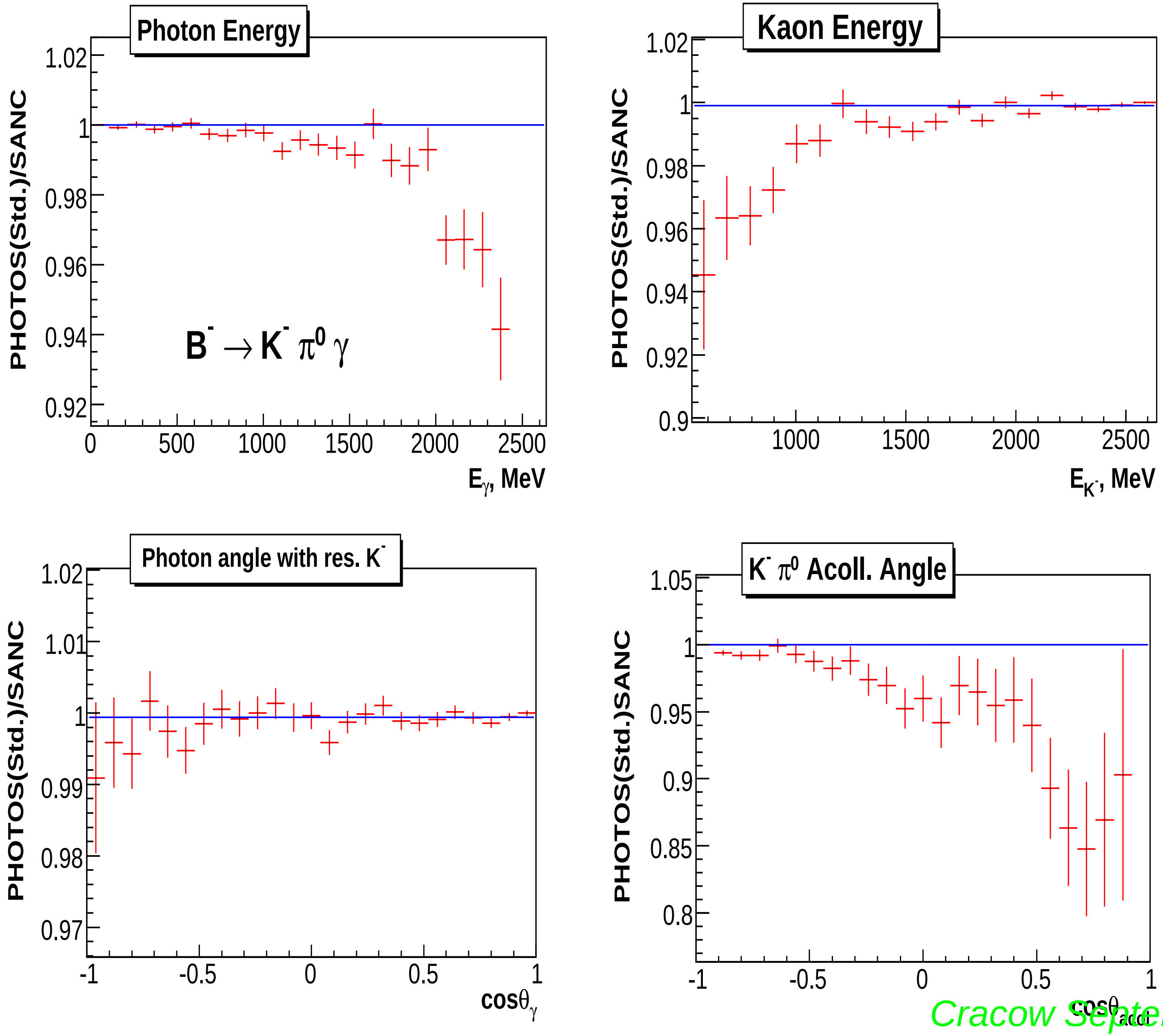

PHOTOS: main properties

$B^- \to \pi^0 K^-$: NLO improved PHOTOS Looks good

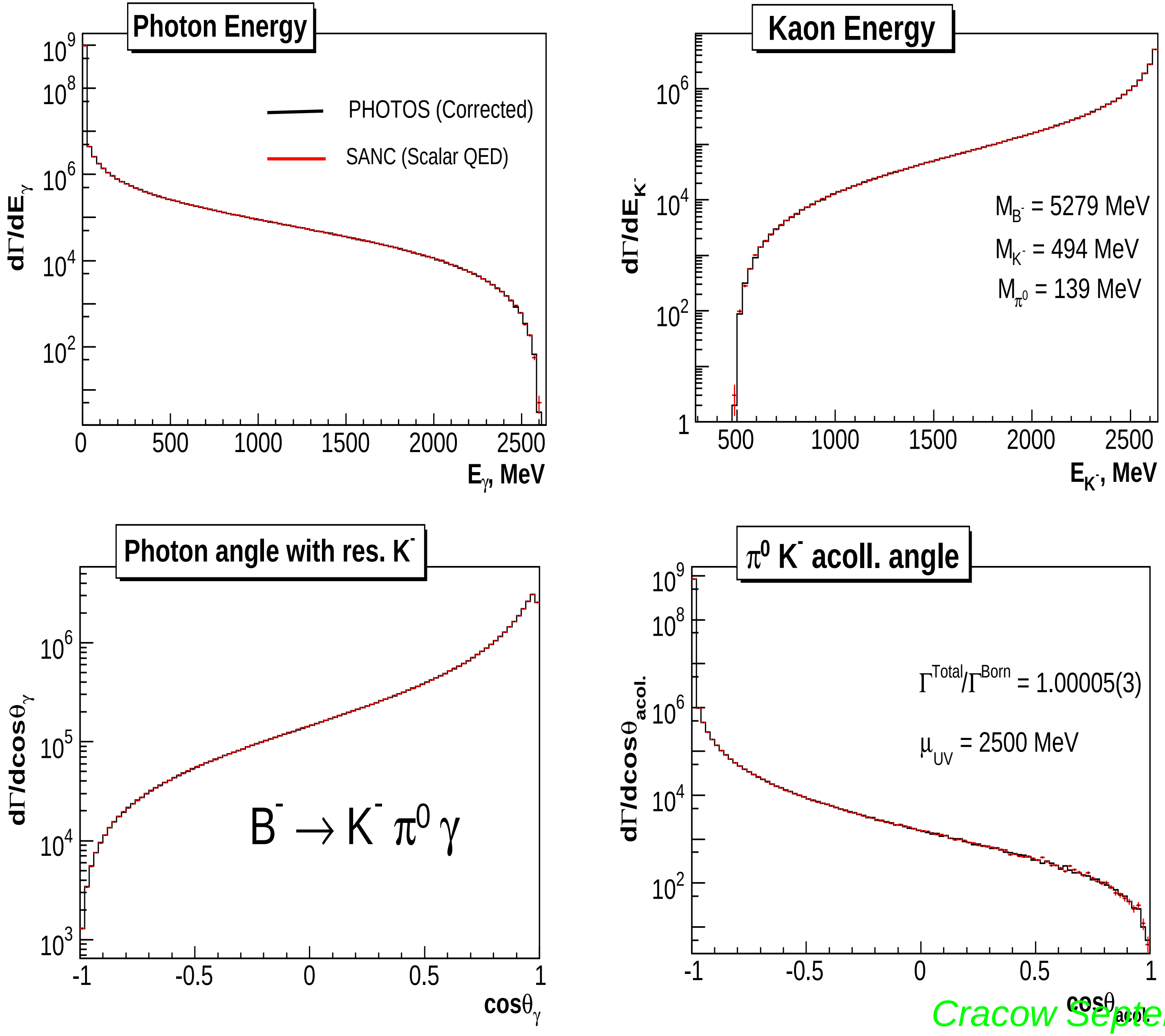

PHOTOS: main properties

$B^- \to \pi^0 K^-$*: NLO improved PHOTOS* ... and is good.

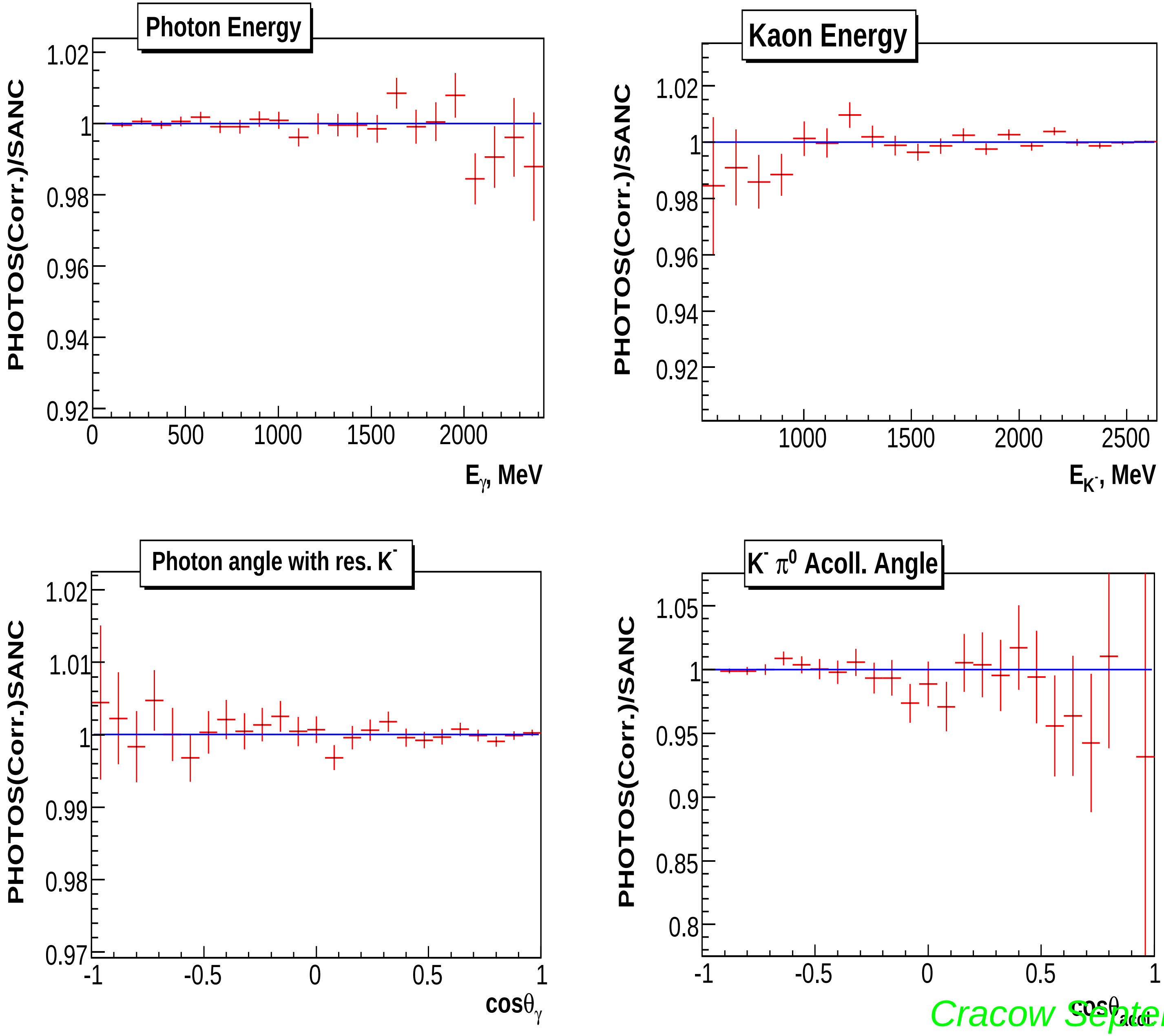

PHOTOS: main properties

$B^0 \to \pi^- K^+$: *standard PHOTOS* Looks good ...

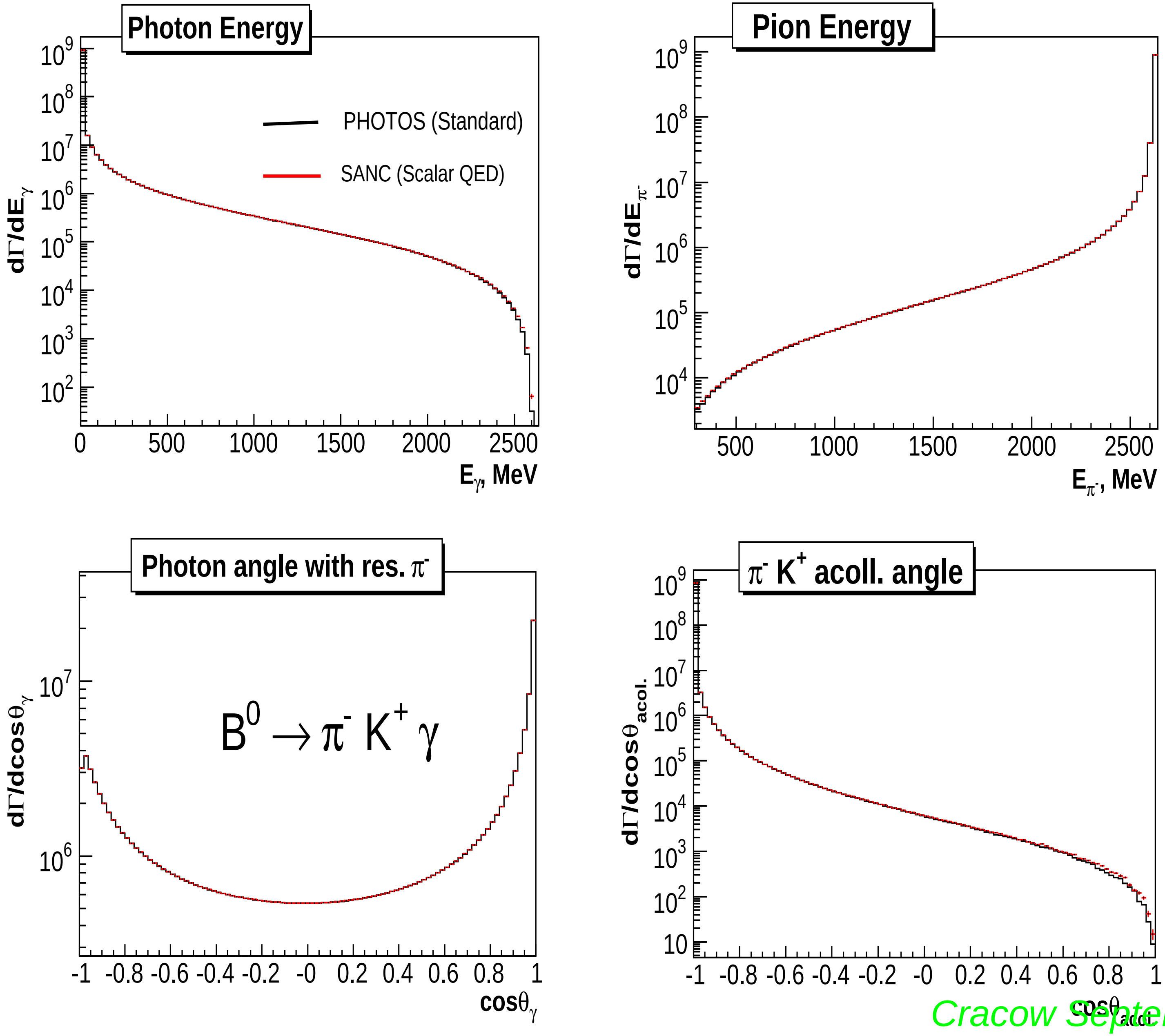

PHOTOS: main properties

$B^0 \to \pi^- K^+$: *standard PHOTOS* ... but not perfect.

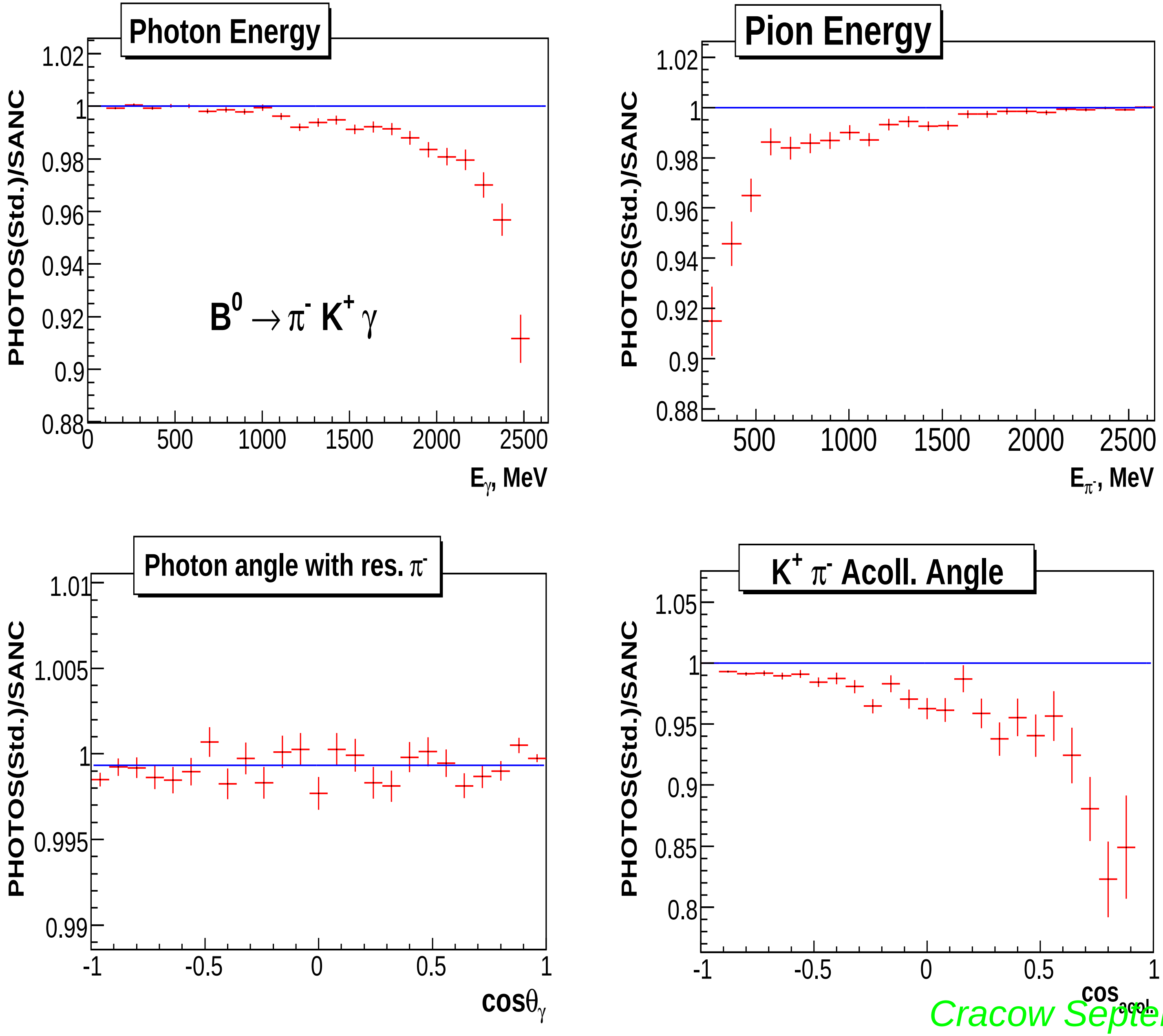

PHOTOS: main properties

$B^0 \to \pi^- K^+$: *NLO improved PHOTOS* Looks good ...

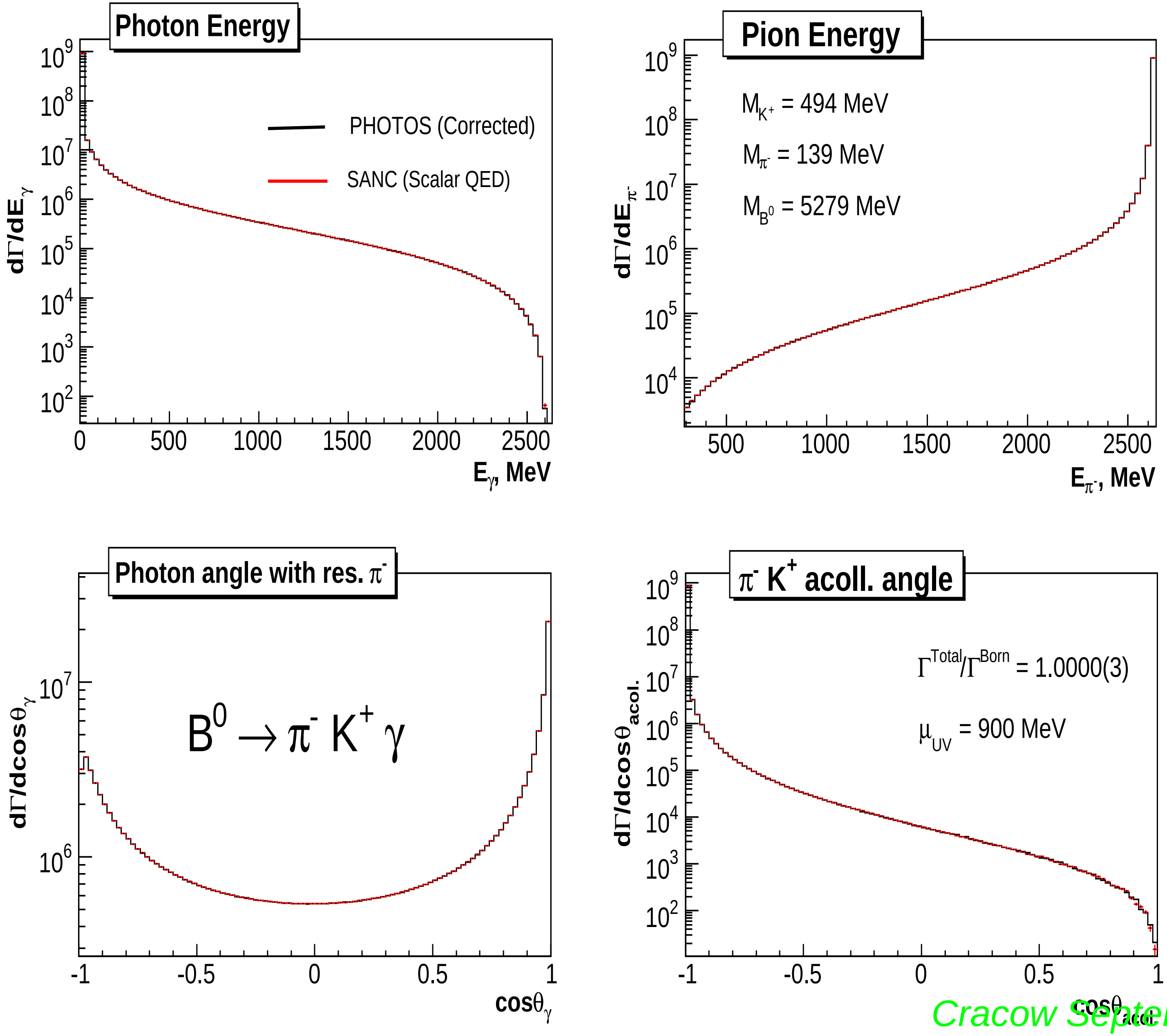

PHOTOS: main properties

$B^0 \to \pi^- K^+$; *NLO improved PHOTOS* ... also perfect !

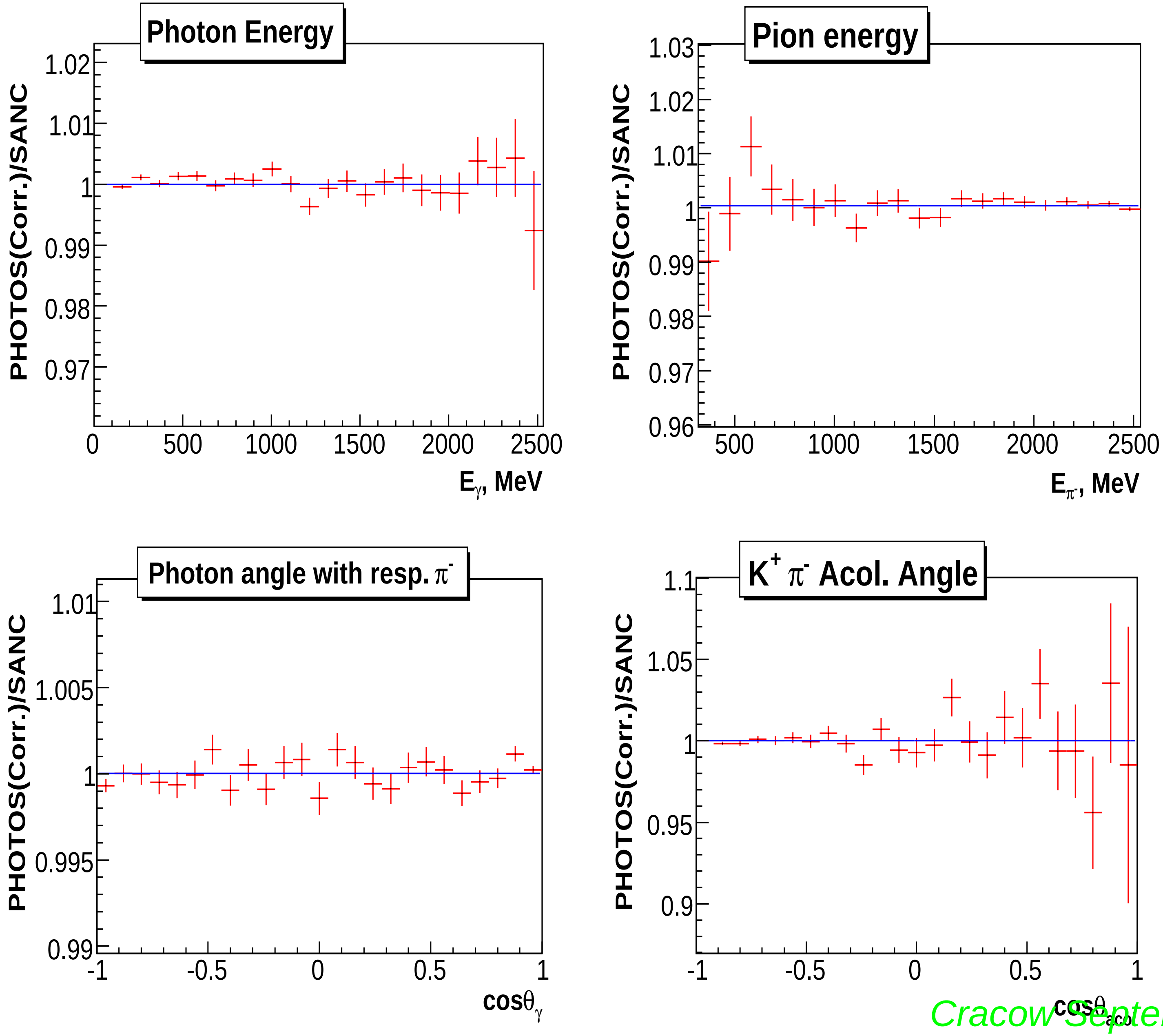

Let us start the discussion from the amplitude of the decay

$$K^-(p) \to \pi^0(q) + e^-(p_e) + \bar{\nu}_e(p_\nu) \tag{7}$$

it reads

$$\begin{aligned} M^c_{\mathrm{Born}} &= \frac{e^2 V_{us} F_{K\pi}(t)}{8\sqrt{2} s_W^2} \frac{(p+q)^\mu}{t - M_W^2} \\ &\quad \overline{u}(p_e, \lambda_e)\gamma_\mu(1-\gamma_5)v(p_\nu, \lambda_\nu)\,, \end{aligned} \tag{8}$$

where $\lambda_e(\lambda_\nu)$ denote the electron (neutrino) helicity, $F_{K\pi}(t)$ is the form factor and $t = (p-q)^2$. Because of the relatively small mass of the K meson, t is always $\ll M_W^2$ and the amplitude simplifies to

$$\begin{aligned} M^c_{\mathrm{Born}} &= \frac{G_F V_{us} F_{K\pi}(t)}{2} (p+q)^\mu \\ &\quad \overline{u}(p_e, \lambda_e)\gamma_\mu(1-\gamma_5)v(p_\nu, \lambda_\nu)\,. \end{aligned} \tag{9}$$

PHOTOS: main properties

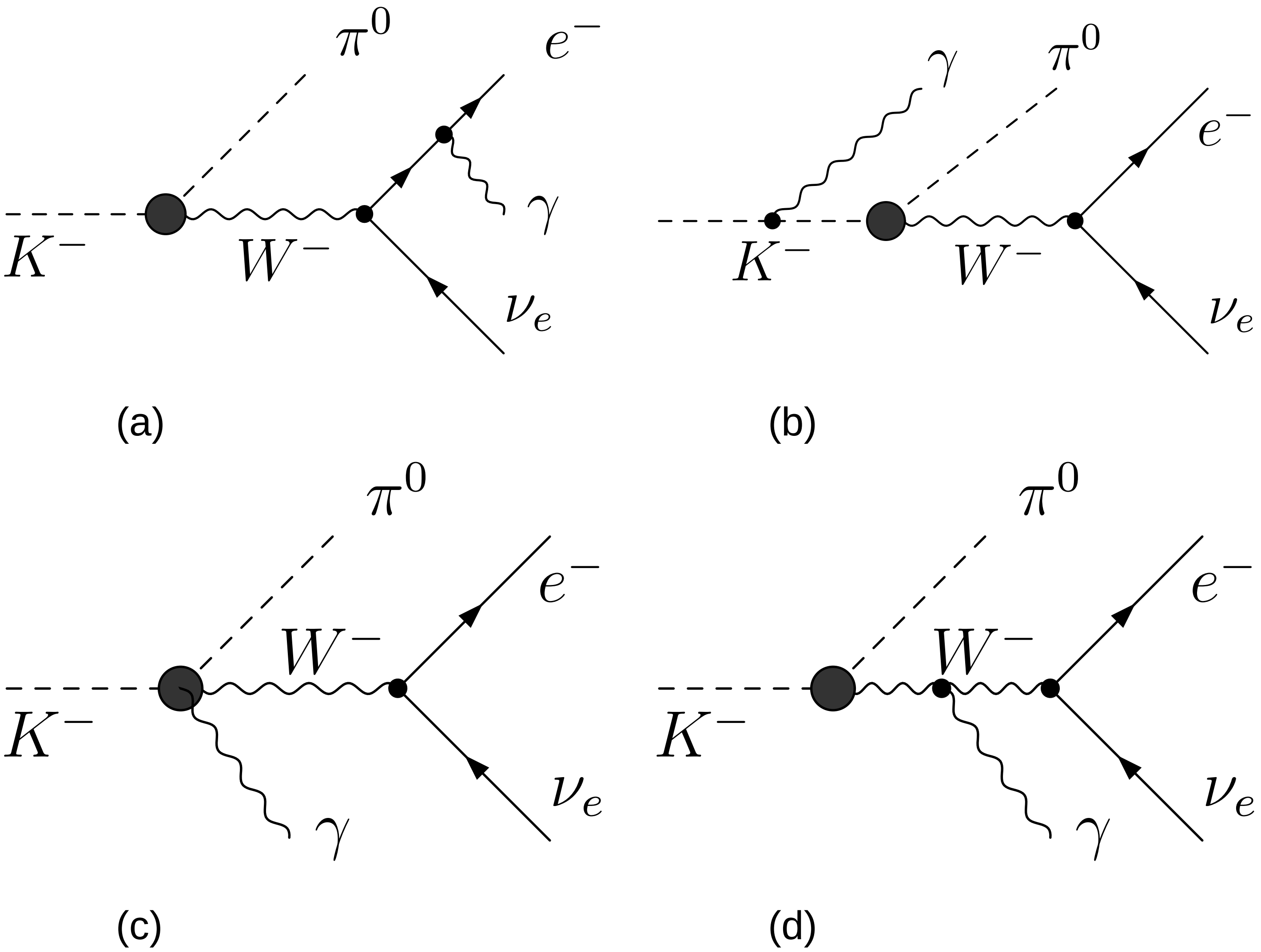

Figure 1: Feynman diagrams of the $K^- \to \pi^0 e^- \bar{\nu}_e \gamma$ decay.

To visualize its factorization properties this amplitude can be expressed as a sum of three gauge invariant terms:

$$M^c = M^c_I + M^c_{II} + M^c_{III} \,, \tag{10}$$

where

$$M^c_I = \frac{G_F V_{us} F_{K\pi}(t)}{2} (p+q)^\mu \left(Q_e \frac{p_e \cdot \epsilon}{p_e \cdot k} - Q_K \frac{p \cdot \epsilon}{p \cdot k} \right) \overline{u}(p_e, \lambda_e) \gamma_\mu (1-\gamma_5) v(p_\nu, \lambda_\nu) \,, \tag{11}$$

$$M^c_{II} = \frac{G_F V_{us} F_{K\pi}(t)}{2} (p+q)^\mu \overline{u}(p_e, \lambda_e) Q_e \frac{\not{\epsilon} \, \not{k}}{2 p_e \cdot k} \gamma_\mu (1-\gamma_5) v(p_\nu, \lambda_\nu) \,, \tag{12}$$

$$M^c_{III} = \frac{G_F V_{us} F_{K\pi}(t)}{2} Q_K \left(k^\mu \frac{p \cdot \epsilon}{p \cdot k} - \epsilon^\mu \right) \overline{u}(p_e, \lambda_e) \gamma_\mu (1-\gamma_5) v(p_\nu, \lambda_\nu) \,. \tag{13}$$

The first term M^c_I consists of the Born-level amplitude times an eikonal factor. The second, M^c_{II}, is free of soft singularity but contributes logarithmically in the collinear limit. Finally the third term, M^c_{III}, is free of both soft and collinear singularities. Hence, formula (10) provides a clearly structured expression of the amplitude.

We need such separation to be prepared for discussion of systematic errors. Terms I II can be used in definition of model independent part of the emission amplitudes. Part III is scalar QED dependent. Each term is separately gauge invariant.

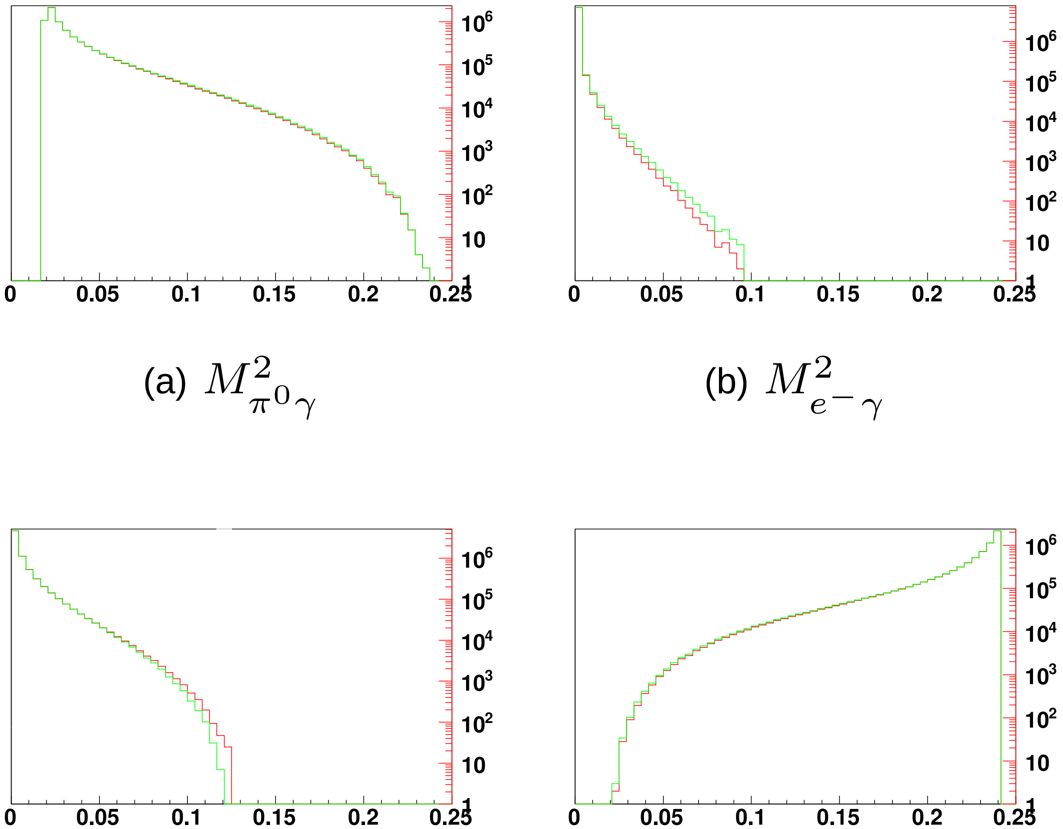

(a) $M^2_{\pi^0\gamma}$ (b) $M^2_{e^-\gamma}$

(c) $M^2_{\bar{\nu}_e\gamma}$ (d) $M^2_{e^-\bar{\nu}_e\pi^0}$

Figure 2: Distributions of scalar Lorentz invariants, in GeV^2 (GeV$^2/c^4$, $c = 1$) units, constructed from the decay products in $K^- \to \pi^0 e^- \bar{\nu}_e$ channel. The most sensitive invariants to photon energy are plotted. The red (darker grey) line is standard PHOTOS, the green is with exact Matrix Element. The fraction of accepted bremsstrahlung events is (7.371 $\pm$0.0027) % in standard PHOTOS run and (7.4127 $\pm$ 0.0027) % when the matrix element is used.

PHOTOS: main properties

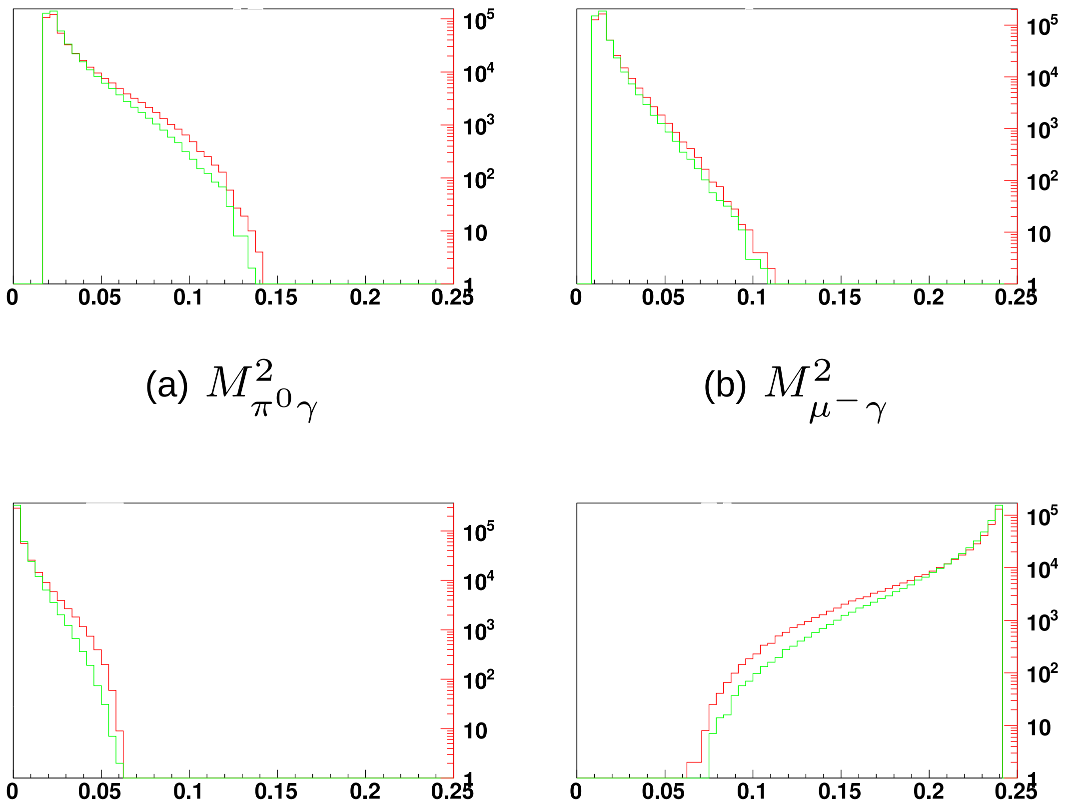

(a) $M^2_{\pi^0\gamma}$ (b) $M^2_{\mu^-\gamma}$

(c) $M^2_{\bar{\nu}_\mu\gamma}$ (d) $M^2_{\mu^-\pi^0\bar{\nu}_\mu}$

Figure 3: Distributions of scalar Lorentz invariants, in GeV^2 units, constructed from the decay products in $K^- \to \pi^0\mu^-\bar{\nu}_\mu$ channel. The red (darker grey) line is standard PHOTOS, the green is with exact Matrix Element. One could conclude that the effect of matrix element introduction is not small in this case. However, only a small fraction of events enter this plot (0.4113 $\pm$ 0.0006) % for standard PHOTOS and (0.4445 $\pm$ 0.0007) % for the case with matrix element.

$\tau \to l\nu\bar{\nu}(\gamma)$ PHOTOS vs TAUOLA

Plot of worst agreement for the channel. Distribution of $\gamma\nu_\tau\nu_\mu$ system mass is shown .

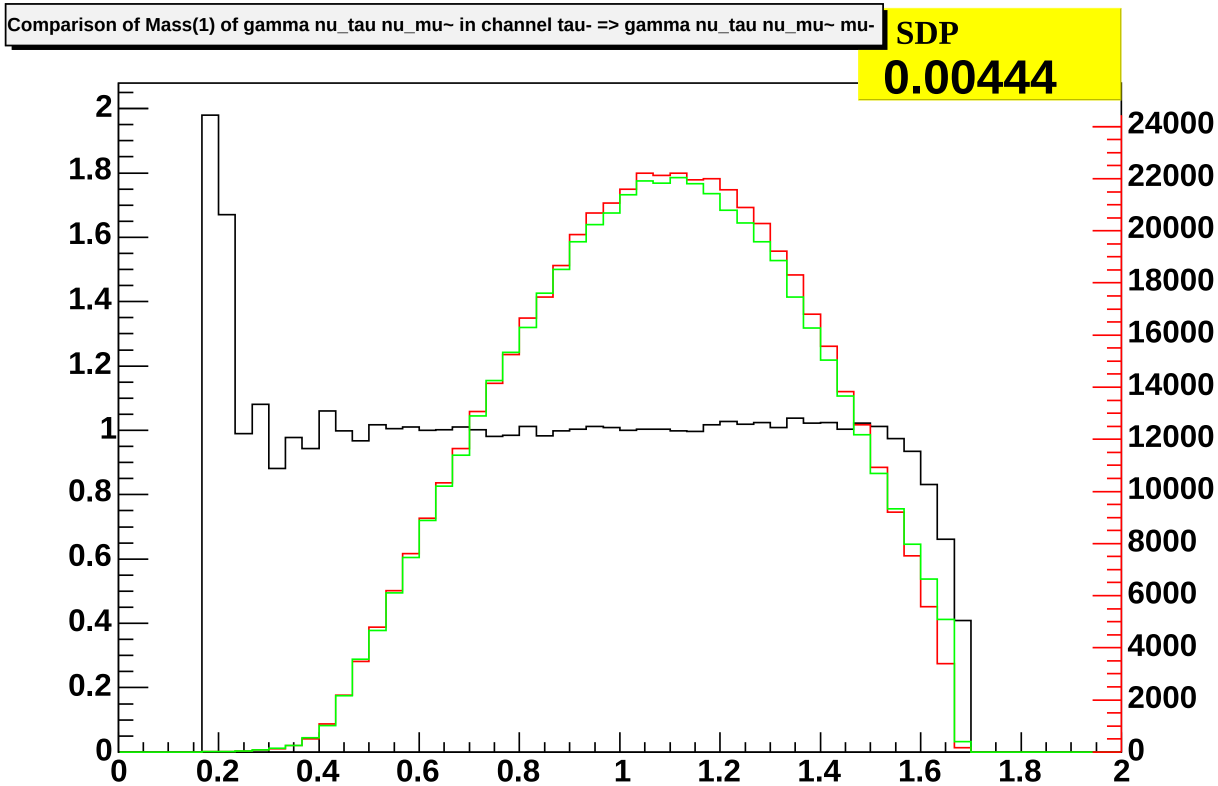

Also the fraction of events with photon above threshold agrees better than permille level.

In TAUOLA complete matrix element, comparison test PHOTOS approximations and design.

Phys. Lett, B 303 (1993) 163-169

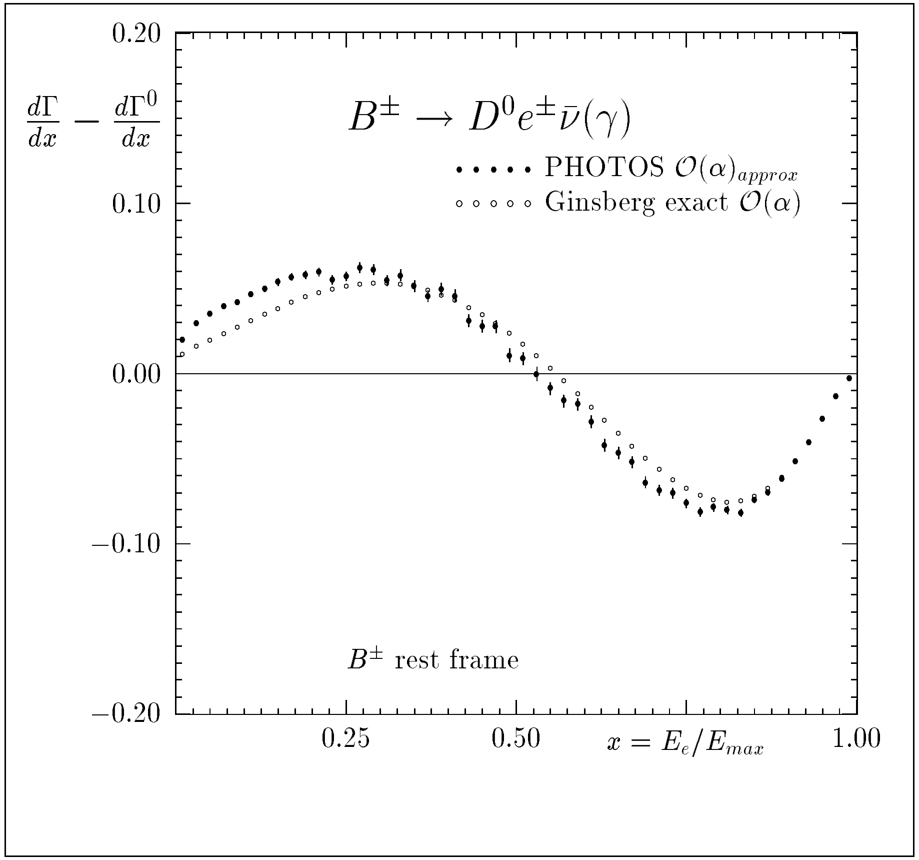

Radiative correction to the decay rate $(d\Gamma/dx - d\Gamma^0/dx)$ for $B^\pm \to D^0 e^\pm \bar{\nu}(\gamma)$ in the $B^\pm$ rest frame. Open circles are from the exact analytical formula [2], points with the marked statistical errors from PHOTOS applied to JETSET 7.3. A total of 10^7 events have been generated. The results are given in units of $(G_\mu^2 m_B^5/32\pi^3) N_\eta |V_{cb}|^2 |f_+^D|^2$, where $N_\eta = \eta^5 \int_0^1 x^2(1-x)^2/(1-\eta x)dx$ and $\eta = 1 - m_D^2/m_B^2$.

- *"QED bremsstrahlung in semileptonic B and leptonic τ decays"* by E. Richter-Was.
- agreement up to 1%
- disagreement in the low-x region due to missing sub-leading terms
- study performed in 1993.

$K \to \pi e \nu(\gamma)$ PHOTOS w/Interf vs Gasser

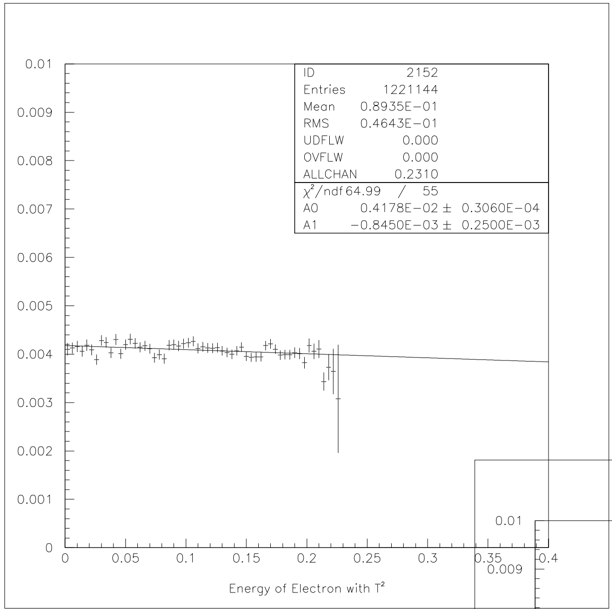

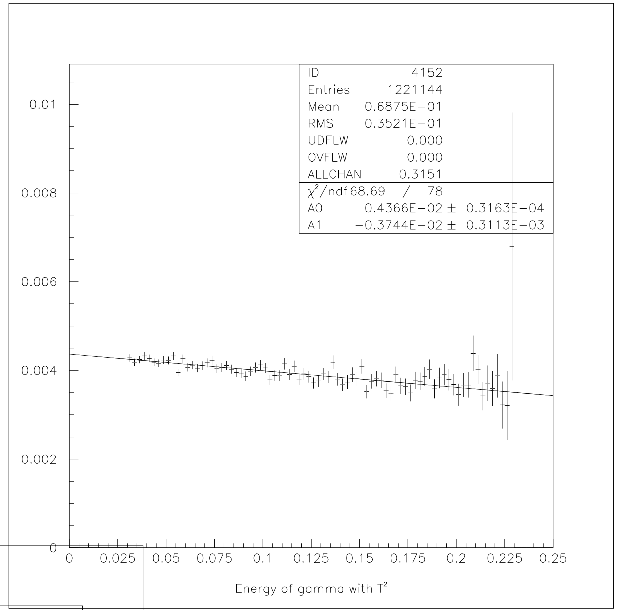

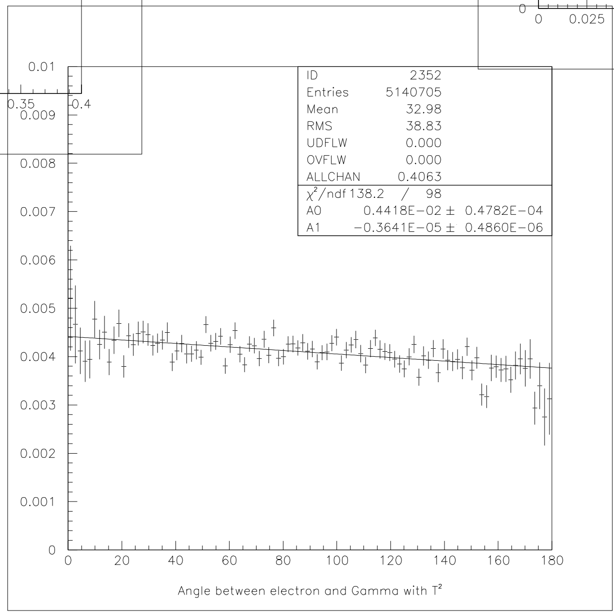

This was OK in 2005

but it is not systematic work.

Events with and without photon:

$R = \frac{\Gamma_{K_{e3\gamma}}}{\Gamma_{K_{e3}}}$	PHOTOS %	GASSER %
$5 < E_\gamma < 15\, MeV$	2.38	2.42
$15 < E_\gamma < 45\, MeV$	2.03	2.07
$\Theta_{e,\gamma} > 20$	0.876	0.96

courtesy of NA48 and Prof. L.Litov

This results can be obtained starting from PHOTOS version 2.13.